EXPERIMENTAL AND ANALYTICAL INVESTIGATIONS OF RECTANGULAR RC COLUMNS RETROFITTED BY FRP UNDER AXIAL AND CYCLIC LOADS

H.Shaheen[1], Y. Hamad [2], I. Shaaban[3], A. Abdelrahman[4] and T. Elrakib[5]

ABSTRACT

Application of fiber reinforced polymers, (FRP), is effective in strengthening circular and square reinforced concrete, (RC), columns. The efficiency of using FRP is considerably reduced when wrapping rectangular columns. Experimental and theoretical investigations are carried out to study the behavior of RC rectangular columns wrapped with FRP sheets under cyclic lateral and axial loading. Eleven RC rectangular columns strengthened by FRP wraps were tested under both cyclic lateral and axial loading. The main parameters investigated in this research were volumetric ratio of FRP, spacing between FRP layers, axial load level, type of FRP sheets, anchorage system of FRP and aspect ratio of columns. Finite element analysis was carried out to predict the response of the tested columns. In addition, a simplified approach, based on a developed numerical computer program, for predicting the curvature ductility factor of FRP retrofitted columns subjected to cyclic loading is reported. The approach was validated by comparing its results with those obtained experimentally. It is concluded that behavior of rectangular columns subjected to cyclic lateral load is significantly enhanced when wrapped with FRP. The proposed approach can be used to predict both the ductility and strength of FRP wrapped rectangular columns.

Keywords: Anchorage, CFRP, Columns, Cyclic Loading, Ductility, FEA, Seismic, Strengthening.

INTRODUCTION

Reinforced concrete, (RC), columns designed according to older seismic design provisions may suffer from structural problems such as inadequate shear strength, flexural strength, insufficient lap splice length and ductility of columns. As a result, retrofitting of such RC columns is vitally needed for buildings located in seismic zones. Proven as an effective technology for alleviating this problem and for enhancing the seismic performance of concrete columns, both steel and RC jackets have been widely implemented for seismic

[1] Prof. of Reinforced Concrete, Housing and Building Research Center, Egypt
[2] Prof. of Reinforced Concrete, Faculty of Engineering, Zagazig Univ., Shoubra, Egypt
[3] Prof., Faculty of Engineering, Zagazig Univ., Shoubra, Egypt
[4]Associate Prof., Structural Engineering Dept., Ain Shams University, Egypt
[5] Assistant Researcher, Housing and Building Research Center, Egypt

retrofit. The increase in the inertia of the strengthened columns due to application of thick jackets will result in an increase in the seismic loads on the structure. Recently, use of advanced composite materials such as carbon and glass fiber reinforced polymers, (CFRP and GFRP), jackets for columns have shown great potential to be a viable alternative to conventional methods. The lightweight, high strength, corrosion resistance and more importantly the negligible changes in the concrete member dimensions make such materials most suitable for retrofitting. Most of the previous work was applied on small columns, circular columns or columns subjected to axial loading only [1], [2]. Rectangular columns, with aspect ratio up to 1 to 5, represent the vast majority of columns used in buildings.

This paper investigates the performance of rectangular RC columns wrapped by FRP sheets and subjected to a combined axial compression and cyclic flexural loading. Rectangular RC columns with aspect ratio of 1 to 3 were tested under constant axial load and increasing cyclic lateral load up to failure. CFRP wraps were applied using different volumetric ratios, spacing and with or without anchors. Axial load level, type of FRP sheets and aspect ratio of the columns were also varying parameters in the study. The displacement ductility, strength, stiffness and energy dissipation capacity were evaluated and compared to optimize the design technique of retrofitting.

Finite element analysis, (FEA), was used to predict the behavior of the tested columns. Despite that FEA was proven to be a valid method for capacity prediction of such columns, the technique is lengthy and need researchers rather than engineers to carry out. Therefore, a method for analysis and design of concrete columns retrofitted by FRP is needed. This paper also presents a simplified approach, based on a developed numerical computer program, for predicting the curvature ductility factor of FRP retrofitted columns subjected to cyclic loading. The results obtained using this approach were compared with the experimental results carried out in this investigation. In addition, the curvature ductility factor was predicted for other available experimental results in the literature in order to verify the developed approach. A good agreement between the predicted and measured behavior using the FEA and the simplified approach was achieved.

TEST PROGRAM

The experimental test program includes eleven specimens with rectangular cross section designated as C1 to C11. The columns have a total height of 2300 mm with different cross sections, as given in Table 1. Nine columns had a cross section of 150 x 450 mm and two columns had cross sections of 150 x 300 and 150 x 150 mm. The columns were tested horizontally under constant axial load combined with increasing cyclic lateral load. Each column consisted of the right part of 1300 mm long and the left part with a length of 700 mm and a beam stub in the middle as shown in Fig.1. The right part of each specimen represented the test portion. It simulated a column at a mid-floor extending from the beam-column connection to the point of inflection. The beam stub, which was heavily reinforced, was the point of application for the lateral load. The dimensions of the beam stub were chosen so that the failure would occur in the column rather than at the joint. The left portion was also heavily reinforced and provided with two 6mm thick steel plates, which were anchored to the specimen by steel bolts of 16 mm diameter, in order to force hinging into the right part and thereby reducing the amount of instrumentations needed. The longitudinal reinforcement ratio of the columns, in the right part, was kept 1% and the bars were uniformly distributed around the perimeter. Steel stirrups were 6mm diameter bars every 150 mm with a volumetric ratio of 0.3%. For the left part, stirrups were 8 mm diameter bars every 100 mm.

FRP laminates were applied to strengthen the columns C2 through C11 with different schemes. The thickness of CFRP laminates was 0.11 mm, while its tensile strength and modulus of elasticity were 2400 MPa and 240 GPa, respectively. For GFRP laminates, the thickness was 0.135 mm, while the tensile strength and modulus were 1700 MPa and 65 GPa, respectively. The characteristic compressive cube strength of the concrete after 28 days, f_{cu}, was 25 MPa while the yield stress of the steel was 430 MPa for the longitudinal reinforcement and 310 MPa for stirrups.

CFRP sheets were wrapped after the concrete had reached an age of 28 days. The wrapping procedure included surface preparation of the columns using a manual hammer and rounding the corners of the columns with a radius of 15 mm, followed by a blower to remove the loose particles. Epoxy grout was used in leveling the concrete surface at the rough locations and around the sharp corners. Epoxy adhesive was mechanically–mixed and applied evenly on the surface using a roller. CFRP sheets were carefully hand–laid to achieve a wrinkle-free surface and provide a complete wrapping of the columns.

Details of Test Specimens

The properties of the tested specimens are given in Fig.1 and Table 1 and summarized as follows:

- The control specimen C1 was subjected to a constant axial compression load of $0.15f_{cu}A_c$ up to failure, where A_c is the cross sectional area of the column. This axial compression load was kept constant for all specimens except for C7 and C8.
- Specimens C2 and C3 were wrapped in the transverse direction with two and one layers of CFRP laminates with 100 mm width, respectively. The clear distance between laminates was 100 mm and the volumetric ratio of CFRP was 0.2 and 0.1% for the two specimens.
- Specimen C4 was wrapped with one layer of CFRP with zero spacing between the layers. The volumetric ratio of FRP was 0.2%.
- Specimen C5 was wrapped with one layer of CFRP as for specimen C3. Steel plates of 50mm width, 190mm length, 12mm thickness and 240 MPa yield stress, were used to anchor the laminates. The plates were discontinuous to eliminate the contribution of the steel plates in the flexural capacity of the columns and yet to provide anchors to the laminates (see Fig.1).
- Specimen C6 was wrapped in the transverse direction with two layers of GFRP. The GFRP laminates were designed to have the same strength compared to CFRP sheets used in specimen C3. The tensile strength of one layer of CFRP equals approximately that of two layers of GFRP based on the manufacturer's data.
- Specimens C7 and C8 were wrapped with the same scheme as for C3, however, they were subjected to compressive stresses of 40% and 0% of f_{cu}, respectively.
- Specimens C9 and C10 were used to study the effect of aspect ratio of the columns' cross-section on its seismic behavior. Cross-sections of dimensions 150x300 and 150x150 with aspect ratios of 2:1 and 1:1 were used for the two columns, respectively. Both specimens had the same retrofitting scheme as of C3.
- Specimen C11 had the same CFRP aspects as of C3 but with an anchorage system consisted of CFRP anchors. Holes were drilled in the predetermined locations of the wraps with diameter of 12 mm penetrating the width of the column. The holes were cleaned with a blower and the fiber anchors were installed in the holes by rounding it over a hollow probe. The probe was pushed through the holes and then the probe was removed after

installing the anchor. The anchors were subjected to a small tension force by equipment especially made to straighten the fibers. Epoxy resin was injected into the holes through the rounded FRP. A very fast action adhesive was used to fix the straight anchors with the concrete surface and then the equipment was removed. The ends of the fibers were bent over the concrete surface by spreading them in a fan shape and epoxy resin was applied. CFRP layers were applied on the top of the fiber anchors as shown in Fig.2.

Instrumentations

Two linear variable differential transducers (LVDTs) with a stroke of ± 200 mm and sensitivity of 0.1 mm were mounted at the top and bottom of the critical section for each column adjacent to the stub. The LVDTs were used to measure the concrete strain and the average section curvature over 200 mm length in the plastic hinge region. The lateral displacement was measured using an LVDT of ±100 mm stroke and 0.1 mm sensitivity. Four electrical strain gages were mounted on the longitudinal and transverse reinforcement of each specimen, in addition to six electrical strain gages attached on the FRP sheets.

Test Setup and Procedure

Two independent reaction frames were used in the testing setup, as shown in Fig.3. The first frame was a 2000 kN double portal, open reaction frame, while the second frame was a 3000 kN, closed horizontal reaction frame. The lateral reversed cyclic displacement was applied at the stub of the beam-column joint using a double acting hydraulic cylinder of 600 kN capacity in compression and 400 kN capacity in tension. The hydraulic cylinder was attached to the cross girder of the double portal frame. The cylinder was equipped with a tension/compression load cell of ± 680 kN capacity to measure the lateral load. The lateral load was transmitted to the specimen by two rigid plates located at the top and bottom of the stub and tied together with four threaded bars. The axial compression load was applied by a manual hydraulic cylinder of 900 kN capacity. At the beginning of each test, the required axial load was applied at the target value and kept constant throughout the test. The cyclic lateral load was applied in displacement control according to the history shown in Fig.4.

OBSERVED BEHAVIOUR

The test specimens were loaded to failure and the observed behavior in terms of cracking, modes of failure, moment-curvature hysteretic response were recorded. For the control specimen, C1, a drop in the flexural strength occurred at cycle Number “4” and the specimen failed in a brittle shear failure mode. A major diagonal tension crack appeared at a lateral load level of 114.0 kN and extended up to failure as shown in Fig.5. Generally, for all the strengthened specimens a major flexural crack initially appeared at the critical section adjacent to the beam stub and extended up to failure. No shear cracks were observed as the FRP wraps prevented diagonal tension cracks even at high lateral displacement. At onset of flexural failure, crushing of concrete, buckling of the longitudinal bars and rupture of the FRP sheets at the corners of the specimens were observed, as shown in Figs. 6 to 8.

The average curvature at the critical section adjacent to the beam stub, Φ, was calculated as follows:

$$\Phi = (\Delta_T - \Delta_B) / (L^* H) \quad \ldots\ldots(1)$$

Where, Δ_T and Δ_B were the displacement measured by the two LVDTs mounted at the top and bottom surfaces of the critical sections respectively, L is the gage length, equal to 200mm and H is the distance between the two LVDTs. The bending moment, M, at the critical section adjacent to the beam stub was obtained as follows:

$$M = 0.42 * P \quad \text{.....(2)}$$

Where P is the lateral force applied by the actuator.

The moment-curvature hysteretic loops are plotted at different stages of loading for each specimen, as shown in Fig.9, except for Column C1 due to a loss of one of the horizontal LVDTs during the test.

For Column C2 with two layers of CFRP, the ultimate moment was 146.37kN-m, which is 1.46 times that of the control column C1. A sudden drop in the flexural strength was observed at cycle number "9" when concrete crushing at the second 100 mm adjacent to the stub occurred. The section curvature at ultimate load was 384.53×10^{-6}/mm. It should be mentioned that the concrete crushing did not occur in the first 100 mm next to the stub due to the high degree of confinement provided by the two layers of CFRP wrapped adjacent to the stub. It was noted that column C2 produced the highest increase in the flexural capacity for the same axial compressive stress of $0.15f_{cu}$, see Fig.(9).

For Column C3 wrapped with one layer of CFRP spaced every 100 mm, the ultimate moment increased slightly after the first cycle. The ultimate moment was 119.6 kN-m, which is 1.20 times that of the control column. The ultimate moment was obtained at cycle number "5" at a curvature of 134.24×10^{-6}/mm. The maximum load remained constant up to cycle number 7 when the load dropped in cycle number 8 to 111 kN. It was noted that column C3 had a low enhancement in the flexural strength due to the small ratio of CFRP.

For Column C4, which was retrofitted with one layer of CFRP sheets with zero spacing between the layers, the flexural capacity was 138.51 kN-m, which is 39% higher than the control specimen. The maximum load was observed at cycle number "6" with a curvature of 217.86×10^{-6}/mm. The maximum load remained constant at cycles number "7" and "8" when rapid degradation in the strength occurred and the column failed due to crushing of concrete at cycle number "9".

The maximum load was observed at cycle number "5" for column C5 with anchored CFRP wraps. The ultimate moment was 134.0 kN-m, which is 1.34 times that of the control column, obtained at a curvature of 143.25×10^{-6}/mm. Gradual degradation in the strength of the column was observed until the column failed at cycle number "9". The gradual loss in the stiffness of the column is attributed to the steel plates used to anchor the FRP laminates. Unlike other specimens, crushing of the concrete was not observed at the full depth of the critical section adjacent to the beam stub; however, it was limited to the top and bottom 100 mm of the cross section. The concrete core did not crush due to the confinement provided by the steel plates anchorage.

For column C6 with GFRP sheets, two vertical cracks appeared at the end of the third cycle adjacent to the beam stub and 100 mm apart. At onset of failure, rupture of GFRP laminates occurred, crushing of concrete and buckling of the longitudinal reinforcement was observed.

The failure occurred at cycle number "10" and was less explosive compared to specimens with CFRP laminates. The ultimate moment was 127.93 kN-m, which is 1.34 times that of the control column, obtained at a curvature of 225.36×10^{-6}/mm.

Column C7 was subjected to a relatively high axial compressive stresses. C7 had a flexural capacity of 127.93 kN-m, which is the highest capacity compared to other tested columns. The stiffness of C7 was higher than that of other columns due to the higher applied axial load on the column. However, the column failed at much less number of cycles. At the end of cycle number "4", the load-deflection behavior had a sudden drop in the stiffness and strength. On the other hand, for column C8, with no axial force, a vertical crack appeared at the beginning of the second cycle at the critical section and two more inclined cracks appeared at the seventh cycle between the first and second FRP layers. Flexural failure due to crushing of concrete after yielding of steel took place at cycle number "9". The ultimate moment capacity was 97.98 kN-m. The stiffness of C8 was much less than other specimens since there was no axial load applied on the column, (see Fig. 9).

Column C9 with aspect ratio of 2 had a vertical crack at the beginning of the third cycle at the critical section and extended up to failure. The moment increased with a relatively high slope up to cycle number "2". The moment increased gradually with less slope up to its maximum value at cycle number "8". Failure took place at cycle number "12", as shown in Fig.7. For Column C10, which had a square cross section, a vertical crack appeared at the beginning of the fourth cycle at the critical section and another crack appeared at the sixth cycle, 100 mm apart from the first crack. Fat hysteresis loops are observed due to the goof confinement of the square columns. FRP sheets did not rupture at failure, but two longitudinal steel bars of the column were ruptured. Again, this is due to the confinement provided by the FRP sheets. Unlike other test specimens, concrete of C10 did not crush (see Fig. 9).

Column C11 with FRP anchors had its maximum flexural capacity at cycle number 5. At cycle number 9, the column failed due to rupture of FRP sheets. The gradual degradation in the lateral strength after reaching the ultimate load is attributed to the used fiber anchorage system (see Fig. 9). The maximum moment was 125.16 kN-m, occurred at a curvature of 151.96×10^{-6}/mm.

DISCUSSION OF THE RESULTS

The relationship between the peak load at each cycle and the corresponding lateral displacement is presented for the tested columns in Figs.10-13. The ultimate moment capacity, (M_u) and the corresponding curvature (Φ) in addition to both the yield and ultimate curvatures, (Φ_y) and (Φ_u), respectively, of each column are also reported in Table 2. It can be seen from Fig. 10 that for columns with the same dimensions and subjected to axial stress of 0.15 f_{cu}, increasing the CFRP volumetric ratio improved the overall strength by 20 to 46%. This increase in the flexural strength is attributed to the confinement provided by FRP, which resulted in an increase in the concrete ultimate strength and strain. It should be also noted that the longitudinal reinforcing bars reached the strain hardening, consequently the stress in the steel bars exceeded the yield stress leading to an increase in the overall strength of the retrofitted columns. Comparing specimens C2 and C4 with the same volumetric ratio of CFRP (ρ=0.2%), it can be concluded that increasing the number of layers instead of reducing the spacing between the layers is more effective. C2 with two layers of CFRP and 100 mm spacing had 46% increase in the strength compared to an increase of 37% for C4 with one

layer of CFRP and zero spacing. This is primarily attributed to the larger confinement provided by the extra layer of CFRP. Specimen with two layers of GFRP, C6, had higher strength and deformation at ultimate and experienced more number of cycles before failure than specimen C3 with one layer of CFRP. It should be noted that the tensile force of two layers of GFRP is equivalent to that of one layer of CFRP. This is attributed to the larger strain at ultimate for GFRP sheets.

Fig.11 shows that use of anchorage system to CFRP sheets resulted in better behavior of the strengthened columns. Columns C5 and C11 with steel and fiber anchors had 34 and 25% increase in the flexural strength, respectively, compared to 20% increase in the load for column C3 with no anchor. This indicates that the fiber anchor system needs more development to achieve better results. Comparing columns C4 and C5, it can be also concluded that proper choice of the anchorage system is more feasible than reducing the spacing between sheets.

Fig.12 shows that increasing the axial stress on columns increased the flexural capacity and reduced the deformations. The longitudinal steel yielded for all specimens, however, the number of cycles at which the failure occurs is reduced.

The aspect ratio of the columns has a much bigger influence on the results than other variables included in the study. The ratio between the normalized ultimate lateral strength ($M_u/ f_{cu}\ b\ d^2$) for the tested columns and that of the control column C1 is reported in Table 2. This ratio is used to evaluate the efficiency of the strengthening scheme for columns with different dimensions. Fig.13 shows that the increase in the flexural strength is 104, 45 and 20% for columns C10, C9 and C3 with aspect ratios of 1:1, 1:2 and 1:3, respectively. CFRP ratio of the three specimens was kept constant and equal to 0.1%. The deformations and number of cycles survived before failure are much higher for columns with small dimensions due to the larger confinement provided by FRP. Decreasing the aspect ratio from 1:3 to 1:1 resulted in that the mode of failure had changed from yield of steel followed by crushing of concrete to rupture of steel reinforcement. However, both types of failure were ductile due to large deformations accompanied by yield of steel.

Curvature Ductility Factor

The curvature ductility factor is defined as the ratio between the curvature at failure load, Φ_f, and the yield curvature, Φ_y, as given by equation (3). The failure moment was taken equal to 75% of the ultimate moment on the descending branch on the moment envelope and the corresponding curvature Φ_f was computed accordingly. The yield curvature Φ_y was calculated as the curvature at the intersection of the secant stiffness of a moment equivalent to 75% of the ultimate moment capacity and the tangent at the ultimate moment. This is equivalent to the definition of yield curvature of an elasto-plastic system with reduced cracked stiffness given by [11].

$$\text{Curvature Ductility factor} = \mu_\Phi = \Phi_f/\Phi_y \quad \text{..... (3)}$$

The curvature ductility factors for the tested specimens are given in Table 2. The control column failed in a brittle shear mode, however, the strengthened columns failed in a ductile mode with ductility factors more than 5.8 for columns with axial stress of 0.15 f_{cu}. Column C7, which was subjected to a high axial stress, had a poor ductility performance and the lowest ductility factor of 3.35. This is due to the high axial load level, which normally has a negative influence on the ductility of columns and accelerates strength degradation. It can be

seen from the ductility factors that increasing the FRP reinforcement ratio increase the ductility; however, use of two layers of CFRP (specimen C2) gives better ductility than use of one layer with the same reinforcement ratio (specimen C4). Table 2 shows that column C6, wrapped with two layers of GFRP, achieved a good ductility factor of 9.21, which is 1.58 times that of C3 with CFRP. It was noticed that both columns had the same increase in moment capacity. The overall response of columns C3 and C6 showed that confinement made by GFRP wrapping is more effective, for ductility enhancement, than CFRP providing the same confining force. It is also observed that the ductility of columns C4 with two CFRP layers and no anchors is similar to that of column C5 with steel anchors despite that the C5 has 50% less CFRP wraps. This indicates that using an anchorage system had a positive influence on the moment resisting capacity and ductility of the retrofitted columns. This may be attributed to the fact that using the anchorage systems leads to a reduction in the area of the ineffectively confined concrete at the level of the FRP laminates and consequently increasing the effective lateral confining pressure. Column C11 with fiber anchors exhibited a more ductile behavior than C3 with no anchorage system as well as good energy dissipation. However, the increase in the ductility does not balance the time and effort to prepare the anchors.

It can be noticed from Table 2 that specimen C10 with a square cross section developed significantly improved seismic behavior characterized by achieving the highest value of ductility factor which is 1.8 times that of C3. It also survived more cycles than all the other columns indicating an excellent capability of energy dissipation. It was clearly noted that decreasing the aspect ratio of columns leads to a more effective confinement system provided by the FRP sheets and consequently improving both of the strength and ductility. However, test results conducted in this investigation indicated that the enhancement of the seismic performance of FRP wrapping retrofit for rectangular columns with aspect ratio up to 3 is quite satisfactory.

FINITE ELEMENT MODELING OF THE TESTED COLUMNS

Finite element analysis using “IDARC” computer code is adapted to predict the effect of the different retrofitting schemes on the behavior of RC columns strengthened with FRP under seismic loading. IDARC3 is a code for two dimensional analysis of 3D building systems in which a set of frames parallel to the loading direction are inter-connected by transverse elements to permit flexural-torsional coupling, Kunnath et al (1). The library of the program includes different element types such as beam-column elements, shear walls, inelastic axial elements and discrete spring elements. Effect of confinement on the descending branch of the concrete stress-strain relationship is included. The concrete in tension is linear till cracking, while after cracking, tension cut off was assumed and the stiffness normal to a crack direction was set to be zero. The stress-strain relationship of longitudinal and lateral reinforcement used in the columns was assumed to be a bilinear and tri-linear, respectively. Three hysteresis control parameters are used in conjunction with the nonsymmetrical tri-linear curve to establish values under which inelastic loading reversals take place. The three main parameters represented in the model are stiffness degradation α, strength deterioration ß and bond slip γ. The computer code was modified by Shaaban and Torkey [2] for the analysis of RC elements strengthened with FRP.

The tested columns were modeled analytically using the modified IDARC3. Behavior of the control specimen C1 was predicted as shown in Fig.14. It can be noticed that there is a good

agreement between the experimental and predicted results by the proposed model. However, the predicted maximum load is 278 kN, which is 17% higher than the experimental value. After the maximum load is achieved, degradation of the stiffness as the number of cycles increases is demonstrated in the figure. Fig.15 shows a comparison between the experimental and predicted results of the load-displacement hysteresis loops of typical specimen 'C3". There is also a good agreement between the experimental and predicted results using the proposed model. In addition, the predicted maximum load at each cycle increases gradually from cycle to cycle up to the peak value, 336 kN, which is 18% higher than that of the experimental value. Both ductility and capacity enhancement of RC columns can be seen in the last two figures by adding FRP wraps.

SIMPILIFIED DESIGN APPROACH FOR DUCTILITY ENHANCEMENT

A simplified design approach for ductility enhancement of concrete columns subjected to cyclic loading and retrofitted with FRP is developed using a computer program. The experimental results showed that the concrete in the compression zone of the tested specimens was effectively confined since FRP wraps achieved strains up to 50% of its ultimate value reported by the manufacture. The confining pressure improved both ultimate compressive strain and strength of concrete and consequently increased the moment and ductility capacity of the tested columns. Therefore, the nonlinear stress-strain behavior of confined concrete and bilinear stress-strain behavior of steel were considered in the model. Both creep and shrinkage of concrete as well as shear deformation were ignored. Concrete in tension and bond-slip of steel reinforcement were also ignored in the model.

Two stress-strain models of the confined concrete proposed by Mander et al.[3] and Mirmiran[4] were adopted. Mander et al.[3] developed a unified stress-strain model for axially loaded steel-reinforced concrete members with either circular or rectangular sections. Seible et al.[7] proposed a modification to account for the different behavior of FRP-confined concrete. For modeling purpose, the effective circumferential FRP failure strain ε_{uj} was estimated according to equation (5). Based on the experimental work in the current investigation and verified by others [10], the value of k_m may be taken as 0.50.

$$\varepsilon_{uj} = k_m \quad \varepsilon_{tuj} \qquad \text{..... (4)}$$

where ε_{tuj} is the ultimate tensile strain of the jacket.

Although widely used for steel and FRP jacketed RC columns, Mander's model [3] was originally developed for conventional RC columns. It is therefore based on an elastic, perfectly plastic behavior of the jacket, and hence considers the confining pressure constant after the concrete has reached its compressive strength. While this may be representative of steel-jacket columns, it does not hold true for FRP-jacketed columns. FRP behave linear elastically until failure and the confining pressure increases continuously, Shahawy [5].

The analytical bilinear stress-strain model developed for RC columns wrapped with FRP jackets by Mirmiran et al.[4] was also adopted. The model accounts for the continuous interaction between the concrete and the confining FRP due to increase in the lateral strains of concrete. The model was derived on the basis of experiments performed on circular columns. On the contrary to circular columns, the lateral confining pressure differs in the two axes of rectangular columns. This was reflected in the calculation of the confining pressure proposed

by Shahawy et al.[5] to apply the model for rectangular columns. Unlike the model of Mander, the FRP-confined concrete shows an ever-increasing stress-strain relationship due to the continuously increasing confining action of FRP material.

Strain compatibility approach was applied to the tested specimen using the stress-strain characteristics of the confined concrete. A computer program was made to perform the iterations. Table 3 shows a comparison between the predicted and experimental curvature ductility factor for the tested columns. The predicted ductility factors agreed well with the measured values using the proposed models of Mander[3] and Mirmiran[4]. The model of Mirmiran[4] gave slightly more accurate results with an average ratio of 1.20 and standard deviation of 0.129. Applying Mander's model, the average ratio was 1.17 and the standard deviation was 0.186. It can be seen from Table 3 that the calculated curvature capacities were always reasonably smaller than the actual values, except for column C8 without axial loading and applying Mander's model. The conservative results is attributed to the predicted value of ε_{cu} given by Seible[6] which is directly affects the value of curvature at failure. It can be also observed that the ratio between the measured and predicted ductility factor for column C7subjected to high axial stress (0.4 f_{cu}) was the highest among all the tested specimens.

Verification of the simplified model

The proposed model was applied to columns tested by Seliem et al. [7] for verification. Tests were carried out on seven RC columns wrapped with CFRP and GFRP under both axial and cyclic loading. Five columns had rectangular cross section and the other two columns were circular. The unconfined concrete strength, based on cubic strength varied from 37.8 MPa to 45.6 MPa. The reported hoop strength and elastic modulus of the CFRP wraps were 876 MPa and 72.4 GPa, respectively. For GFRP, these values were 575 MPa and 26.1 GPa. The main studied parameters were the shape of the cross section, type of FRP used in retrofitting and the thickness of the jacket. Fig.16 shows a comparison between the predicted and measured plastic displacements. The simplified model used in this research showed good agreement for both models of Mander and Mirmiran with an average ratios of 1.56 and 1.38.

CONCLUSIONS

CFRP wraps showed an excellent enhancement to the overall behavior of the columns including both capacity and ductility. Conclusions can be summarized as follows:

1. All the wrapped specimens failed in a ductile flexural mode instead of the brittle shear mode of the control column.
2. Increasing the CFRP volumetric ratio improved the overall behavior of the column and increased the transverse strength. However, it is more effective to increase the number of layers instead of reducing the spacing between the layers.3.
3. Proper choice of the anchorage system is more feasible than reducing the spacing between sheets. This could be observed from the behavior of columns C4 and C5, which was similar despite that CFRP ratio was 50% less for column C5.
4. For ductility enhancement and providing the same confining force, wrapping with GFRP is more efficient than CFRP. Column with two layers of GFRP had 53% increase in the curvature ductility compared to the column wrapped with CFRP. On the other hand, CFRP wraps provide higher increase in strength due to the fact that it has higher stiffness and strength than the GFRP.

5. The axial load level has a beneficial influence on the moment resisting capacity and stiffness but it has a negative effect on the ductility of the retrofitted columns.
6. As the aspect ratio of columns decreases, the confinement system provided by FRP becomes more efficient and both strength and ductility are improved.
7. Finite element analysis could be used to predict the hysteresis loops of the tested columns. Differences of 18% on the unconservative side were observed between the predicted and measured capacities of the columns.
8. The developed simplified approach can be used successfully to predict the curvature ductility factor of FRP confined columns subjected to axial and lateral loading. Two analytical models, developed in the literature to present the axial stress-strain relation of the FRP-confined concrete up to the failure, were used. The design approach is conservative and showed a good agreement with the test results.

REFERENCES

1. Saadatmanesh, H., Ehsani, R., and M. W. Li "Strength ad Ductility of Concrete Columns Externally Reinforced with Fiber Composites Straps" *ACI Structural Journal*, Vol. 91, No. 4, July-Aug., 1994.
2. Hosny, A., Shaheen, H., Abdelrahman, A., and El-Afandy, T. "Strengthening of Rectangular RC Columns Using CFRP", *M.Sc Thesis*, Faculty of Eng., Ain Shams Univ., 2002
3. Mander, J.B., Priestly M.J.N., and Park R., "Theoretical Stress-Strain Model for Confined Concrete" *ASCE Journal of Structural Engineering*, Vol. 114, No. 8, August 1988.
4. Samaan, M., Mirmiran, A and Shahawy, M., "Model of Concrete by Fiber Composites", ASCE, V. 124, No. 9, Sept., 1998.
5. Shahawy M and Chaalla O., "Performance of Fiber- Reinforced Polymer-Wrapped Reinforced Concrete Columns under Combined Axial-Flexural Loading" *ACI Structural Journal*, July-August 2000.
6. Priestley M. J. N., Seible, F., R., "Seismic Design and Retrofit of Bridges" John Weily Inc., USA, 1999.
7. Seliem, H., Ghoneim, M.,"Seismic Retrofit of RC Columns Using FRP Jackets for Enhanced Flexural Performance" *The Third Middle East Symposium on Structural Composites for Infrastructure Applications*, Aswan, Egypt, 2002.
8. Kunnath, S.K., Reinhorn, A.M. and Loho, R.H., "IDARC Version 3.0" *National Center for Earthquake Engineering Research*, August 1992.
9. Shaaban, I.G., Torkey, A. "Capacity of RC Structural Elements Retrofitted with GFRP under Cyclic Loading" *The International Symposium on Concrete Structures*, University of Dundee, Dundee, Scotland, UK, 2002.
10. Bencardino, Colotti, Spadea and Totaro, "Axial Load-Flexural Moment in Interaction RC Columns with Bonded FRP Materials", *The Third Middle East Symposium on Structural Composites for Infrastructure Applications*, Aswan, Egypt, 2002.
11. Priestly and Park "Strength and Ductility of Concrete Bridge Columns Under Seismic Loading" *ACI Structural Journal*, Jan.-Feb.1987.

Table1 Details of the tested columns

No.	Column dimensions (mm)	No. of FRP layers	Spacing between layers (mm)	Anchorage system	Type of layers	Level of axial compression	Volumtric ratio of FRP ρ(%)
C1	150 x 450	----	----	----	----	0.15 f_{cu}	0
C2	150 x 450	2	100	-----	CFRP	0.15 f_{cu}	0.2
C3	150 x 450	1	100	-----	CFRP	0.15 f_{cu}	0.1
C4	150 x 450	1	0	-----	CFRP	0.15 f_{cu}	0.2
C5	150 x 450	1	100	steel plates	CFRP	0.15 f_{cu}	0.1
C6	150 x 450	2	100	-----	GFRP	0.15 f_{cu}	0.2
C7	150 x 450	1	100	-----	CFRP	0.40 f_{cu}	0.1
C8	150 x 450	1	100	-----	CFRP	0	0.1
C9	150 x 300	1	125	-----	CFRP	0.15 f_{cu}	0.1
C10	150 x 150	1	200	-----	CFRP	0.15 f_{cu}	0.1
C11	150 x 450	1	100	fiber anchor	CFRP	0.15 f_{cu}	0.1

Table 2 Lateral load-displacement and moment-curvature test results for all tested columns

No.	Maximum load and corresponding deformation		Maximum moment and corresponding curvature		Failure cycle	$\frac{(M_u/ f_{cu}\, bd^2)}{(M_u/f_{cu}\, bd^2 \text{ of C1})}$	Curvature (Φ) x10^{-6}/mm		Curvature ductility factor Φ_f/Φ_y
	P_u (kN)	Δ (mm)	M_u KN-m	Φ x 10^{-6} mm			At yield Φ_y	At ultimate Φ_f	
C1	237.1	4.04	99.58	---	4	1	---	----	---
C2	348.5	27.80	146.37	384.53	11	1.46	48.11	426.32	8.86
C3	284.8	18.91	119.61	134.24	8	1.20	45.2	260.57	5.85
C4	329.8	12.10	138.51	217.86	9	1.37	61.26	411.66	6.72
C5	319.1	11.85	134.0	143.25	9	1.34	47.17	304.56	6.44
C6	304.6	12.08	127.93	225.36	10	1.28	31.52	290.50	9.21
C7	384.3	6.0	161.40	45.96	5	1.62	20.35	68.17	3.35
C8	233.3	15.96	97.98	161.92	9	0.98	35.91	312.33	8.74
C9	146.1	20.0	61.34	331.22	12	1.45	46.08	410.62	8.91
C10	44.3	28.10	18.59	365.31	16	2.04	66.25	701.65	10.58
C11	298	12	125.16	151.96	9	1.25	44.76	273.35	6.12

Table 3 Comparison between experimental and predicted curvature ductility

No.	μ_Φ (exp)	Proposed approach based on model of Mander[3]			Proposed approach based on model of Mirmiran[4]		
		$\varepsilon_{cu} x10^3$	μ_Φ (calc)	$\mu_{\Phi\,(exp)} / \mu_{\Phi\,(calc)}$	$\varepsilon_{cu} x10^3$	μ_Φ (calc)	$\mu_{\Phi\,(exp)} / \mu_{\Phi\,(calc)}$
C2	8.84	7.04	6.94	1.27	7.82	7.92	1.11
C3	5.85	5.67	5.14	1.13	5.13	4.85	1.20
C4	6.72	5.81	5.71	1.17	5.05	4.98	1.31
C5	6.44	5.63	5.75	1.12	6.32	6.26	1.02
C6	9.21	7.11	7.16	1.31	6.96	7.36	1.25
C7	3.35	5.77	2.14	1.56	5.31	2.21	1.49
C8	8.74	4.41	10.36	0.86	3.62	7.92	1.10
C9	8.91	5.93	8.51	1.04	5.02	7.31	1.21
C10	10.58	6.53	10.31	1.05	6.01	8.91	1.18
Average value				1.17			1.20
Std. deviation				0.186			0.129

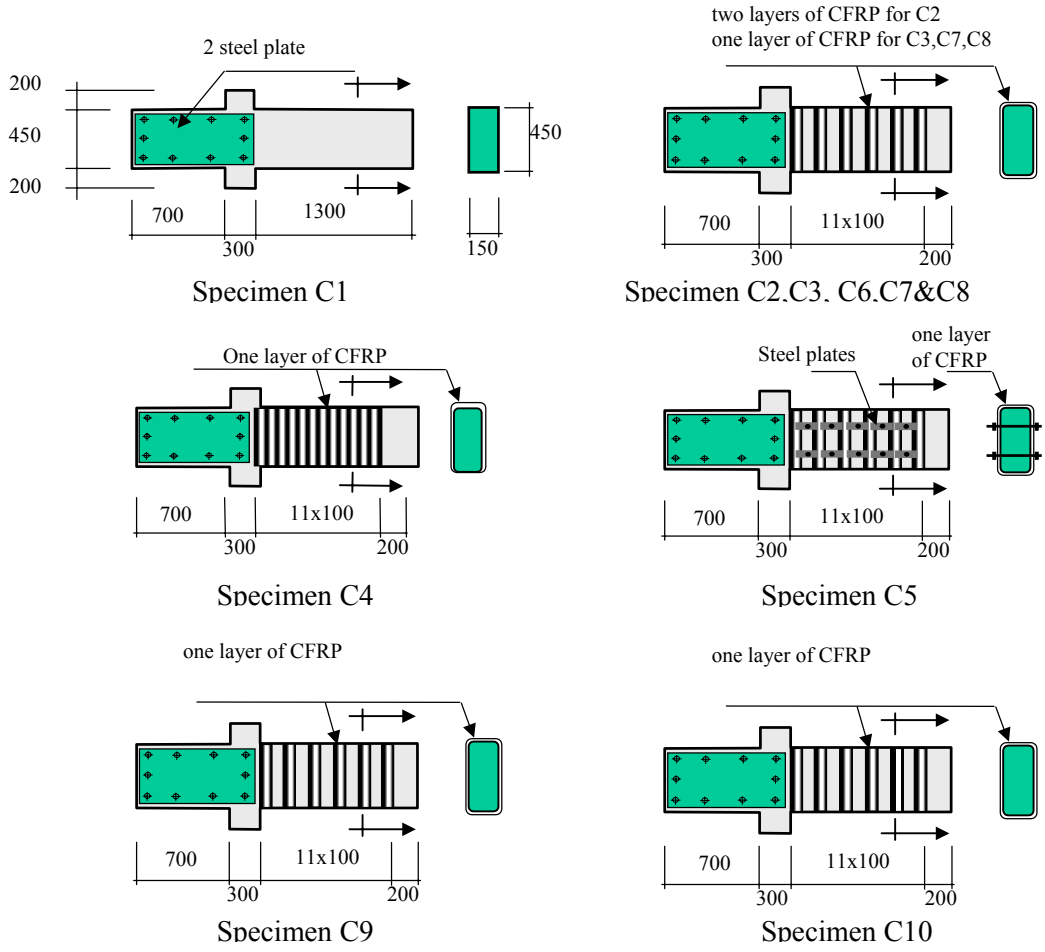

Figure1 Details of test specimens

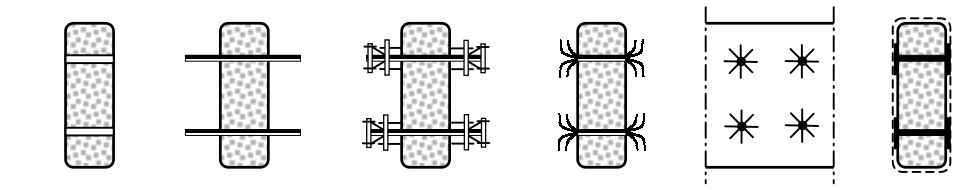

Figure 2-a Installation of FRP anchorage system of Column C11

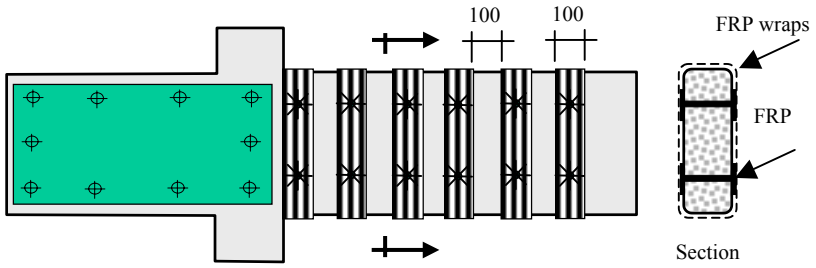

Figure 2-b Details of CFRP wrapping for Column C11

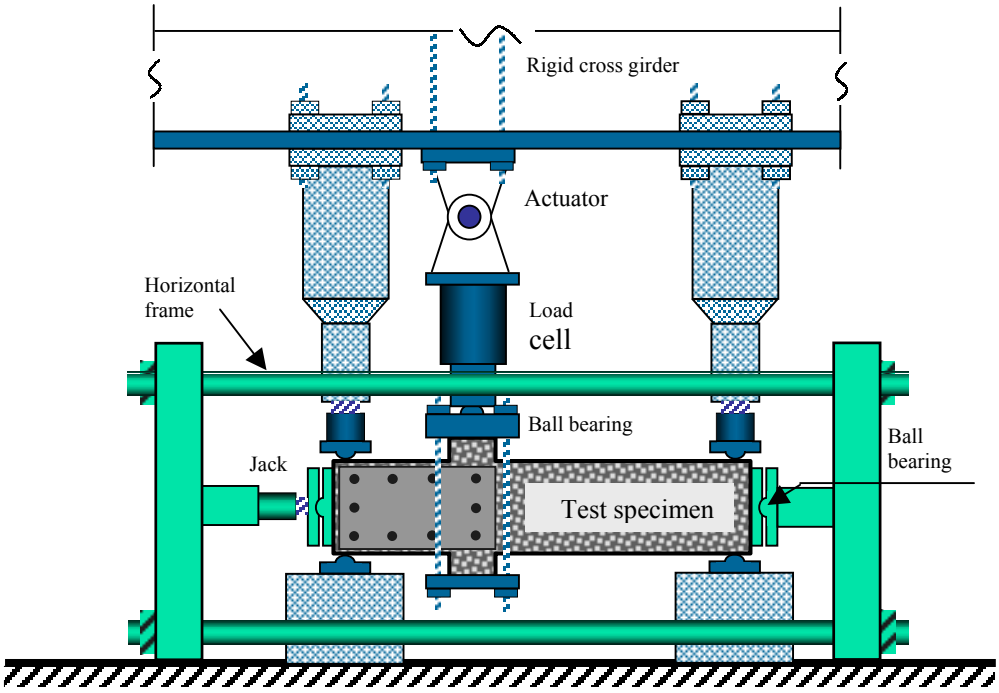

Figure 3a Schematic of test setup

Fig. 3b Test set-up

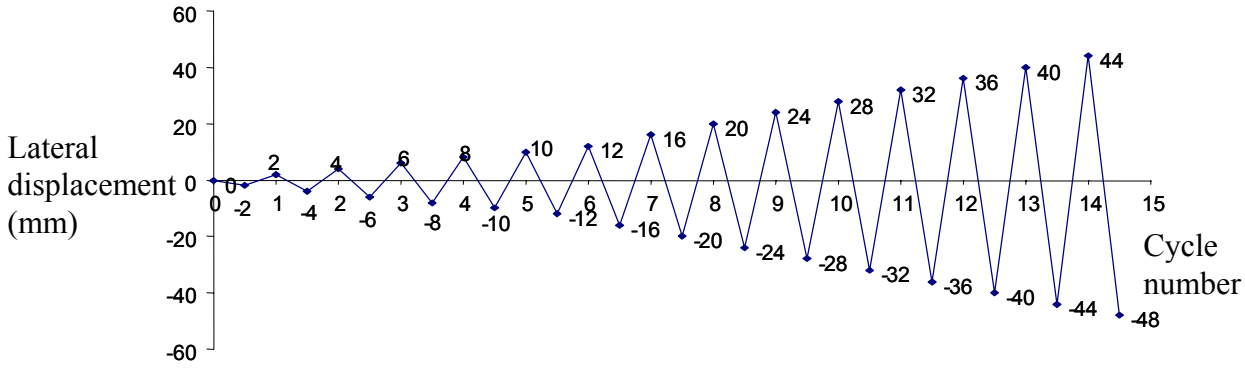

Fig.4 Loading history

Figure 5 Failure of column C1

Figure 6 Failure of column C2

Figure 7 Failure of column C4

Figure 8 Failure of column C6

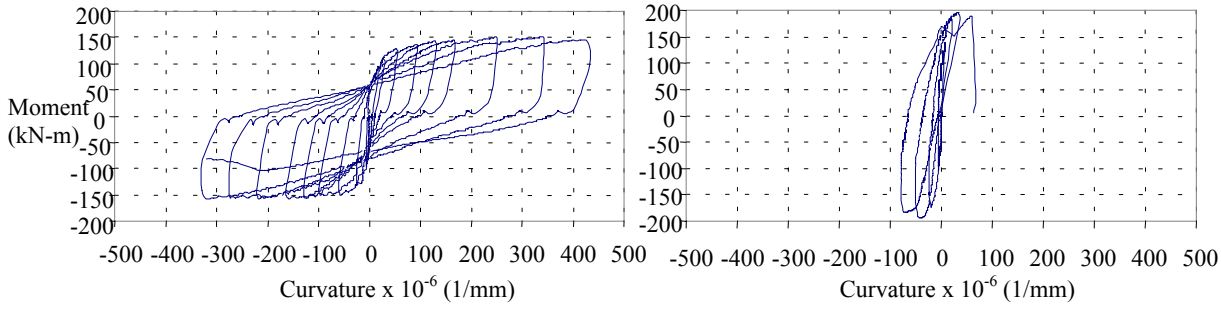

Specimen C6 Specimen C7

Fig. 9 Moment-curvature hysteretic loops of selected specimens

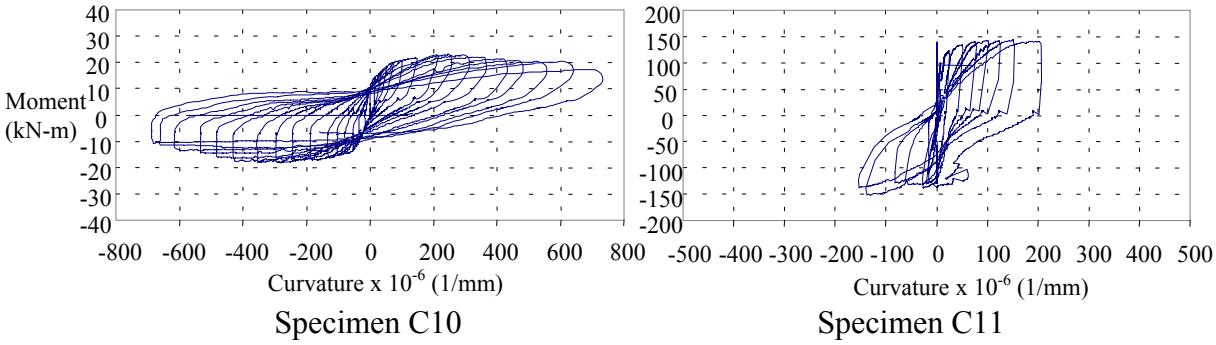

Fig. 9 Moment-curvature hysteretic loops of selected specimens (cont.)

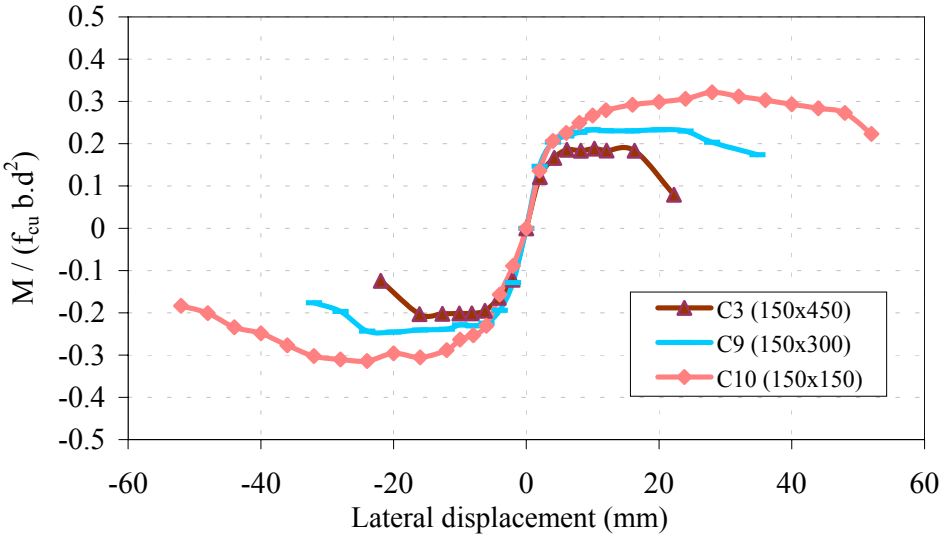

Fig.10 Effect of cross section dimensions of the columns

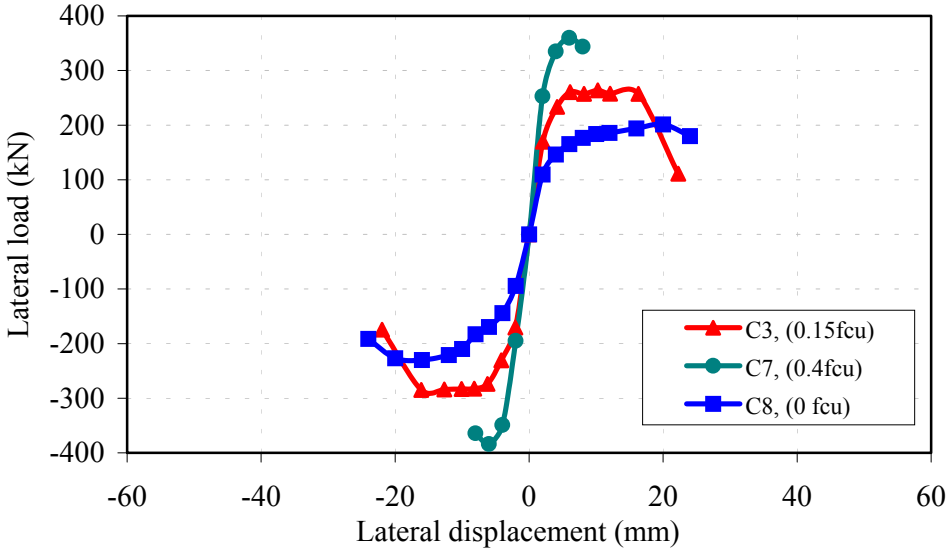

Fig.11 Effect of axial load level

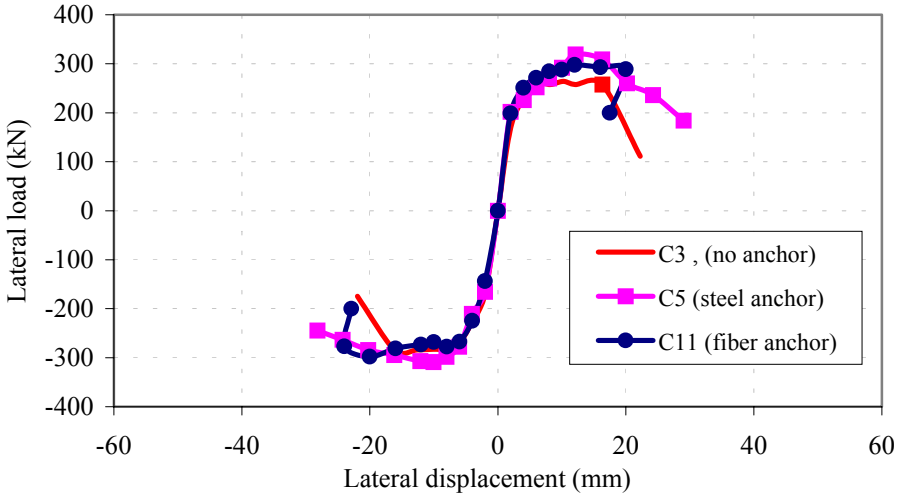

Fig.12 Effect of anchorage system

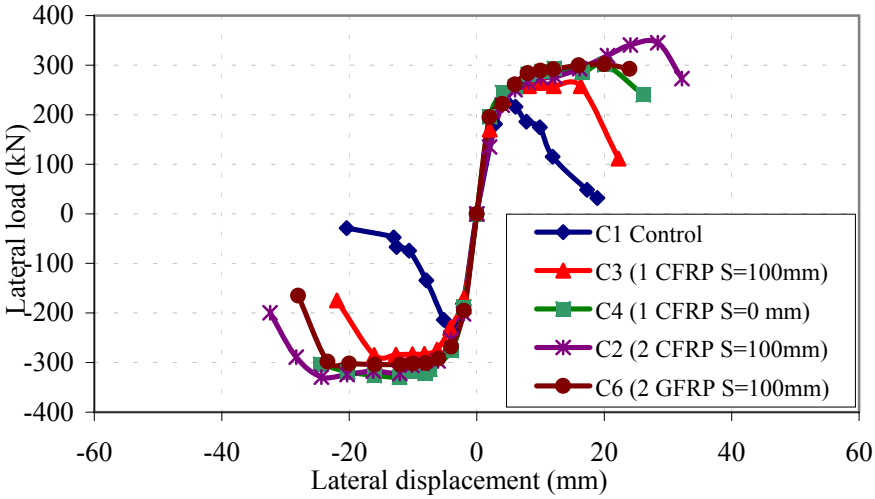

Fig.13 Effect of FRP ratio

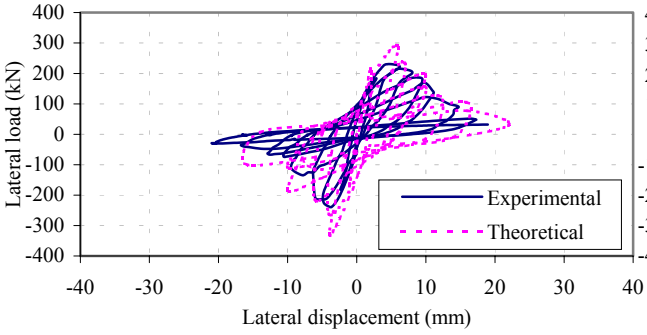

Fig.14 Predicted response of C1 (FEA)

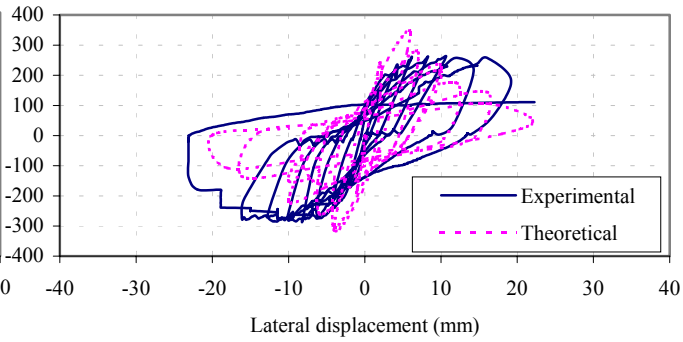

Fig.15 Predicted response of C3 (FEA)

Fig.16 Predicted displacement using simplified approach for columns tested by Seliem [7]